Discovery of Piperidine Ethers as Selective Orexin Receptor Antagonists (SORAs) Inspired by Filorexant

Izzat T. Raheem, Michael J. Breslin, Joseph Bruno, Tamara D. Cabalu, Andrew Cooke, Christopher D. Cox, Donghui Cui, Susan Garson, Anthony L. Gotter, Steven V. Fox, C. Meacham Harrell, Scott D. Kuduk, Wei Lemaire, Thomayant Prueksaritanont, John J. Renger, Craig Stump, Pamela L. Tannenbaum, Peter D. Williams, Christopher J. Winrow, Paul J. Coleman

PII: S0960-894X(14)01364-X
DOI: http://dx.doi.org/10.1016/j.bmcl.2014.12.056
Reference: BMCL 22301

To appear in: *Bioorganic & Medicinal Chemistry Letters*

Received Date: 22 October 2014
Revised Date: 15 December 2014
Accepted Date: 16 December 2014

Please cite this article as: Raheem, I.T., Breslin, M.J., Bruno, J., Cabalu, T.D., Cooke, A., Cox, C.D., Cui, D., Garson, S., Gotter, A.L., Fox, S.V., Meacham Harrell, C., Kuduk, S.D., Lemaire, W., Prueksaritanont, T., Renger, J.J., Stump, C., Tannenbaum, P.L., Williams, P.D., Winrow, C.J., Coleman, P.J., Discovery of Piperidine Ethers as Selective Orexin Receptor Antagonists (SORAs) Inspired by Filorexant, *Bioorganic & Medicinal Chemistry Letters* (2014), doi: http://dx.doi.org/10.1016/j.bmcl.2014.12.056

Discovery of Piperidine Ethers as Selective Orexin Receptor Antagonists (SORAs) Inspired by Filorexant

Izzat T. Raheem,[a] Michael J. Breslin,[a] Joseph Bruno,[e] Tamara D. Cabalu,[c] Andrew Cooke,[a] Christopher D. Cox,[a] Donghui Cui,[c] Susan Garson,[b] Anthony L. Gotter,[b] Steven V. Fox,[d] C. Meacham Harrell,[b] Scott D. Kuduk,[a] Wei Lemaire,[e] Thomayant Prueksaritanont,[c] John J. Renger,[b] Craig Stump,[a] Pamela L. Tannenbaum,[d] Peter D. Williams,[a] Christopher J. Winrow,[b] and Paul J. Coleman.[a]

[a]*Discovery Chemistry,* [b]*Neuroscience,* [c]*Pharmacokinetics, Pharmacodynamics, and Drug Metabolism,* [d]*In Vivo Pharmacology, and* [e] *In Vitro Pharmacology, Merck Research Laboratories, West Point, PA 19486.*

Abstract: Highly selective orexin receptor antagonists (SORAs) of the orexin 2 receptor (OX_2R) have become attractive targets both as potential therapeutics for insomnia as well as biological tools to help further elucidate the underlying pharmacology of the orexin signaling pathway. Herein, we describe the discovery of a novel piperidine ether 2-SORA class identified by systematic lead optimization beginning with filorexant, a dual orexin receptor antagonist (DORA) that recently completed Phase 2 clinical trials. Changes to the ether linkage and pendant heterocycle of filorexant were found to impart significant selectivity for OX_2R, culminating in lead compound **PE-6.** **PE-6** displays sub-nanomolar binding affinity and functional potency on OX_2R while maintaining >1600-fold binding selectivity and >200-fold functional selectivity versus the orexin 1 receptor (OX_1R). **PE-6** bears a clean off-target profile, a good overall preclinical pharmacokinetic (PK) profile, and reduces wakefulness with increased NREM and REM sleep when evaluated *in vivo* in a rat sleep study. Importantly, subtle structural changes to the piperidine ether class impart dramatic changes in receptor selectivity. To this end, our laboratories have identified multiple piperidine ether 2-SORAs, 1-SORAs, and DORAs, providing access to a number of important biological tool compounds from a single structural class.

Introduction

Orexin-A (OX-A) and orexin-B (OX-B) are hypothalmic neuropeptides that are derived by the proteolytic cleavage of a common precursor peptide, prepro-orexin.[1] Exogenous administration of orexin neuropeptides increases locomotor activity and wakefulness in multiple species by signaling through two G-protein-coupled receptors, orexin 1 receptor (OX_1R) and orexin 2 receptor (OX_2R).[2] Maintenance of wake has been demonstrated genetically and pharmacologically to be a key function of the orexin system. Dogs lacking functional OX_2R and rodents whose prepro-orexin gene has been knocked out demonstrate a narcoleptic phenotype with altered sleep/wake cycles and hypersomnolence.[3,4] Post-mortem studies of human narcoleptic patients reveal very few surviving orexin-producing neurons in the hypothalamus, with low-to-absent levels of orexins in the cerebral spinal fluid (CSF).[5] Further, acute blockade of orexin signaling by small-molecule dual orexin receptor antagonists (DORAs) has been shown to dose-dependently promote sleep in rats, dogs, and mice, implicating the key role of orexins in sleep/wake regulation.[6] Recently, several potent DORAs have demonstrated clinical proof of concept for the sleep-promoting effects of orexin blockade for the treatment of primary insomnia (Figure 1).[7] In particular, suvorexant and filorexant are potent DORAs from our laboratories that are under clinical evaluation, and suvorexant (Belsomra) was recently approved by the FDA as the first orexin receptor antagonist for the treatment of insomnia.

PLACE FIGURE 1 HERE.

Figure 1. Representative dual orexin receptor antagonists (DORAs) that have advanced into clinical trials.

Despite the prolific growth in orexin research over the past decade, much remains to be learned about the function of the downstream neurological targets of the individual orexin receptors. Receptor function has often been elucidated through the actions of OX-A and OX-B. OX_1R and OX_2R mRNAs have overlapping but distinct distribution

patterns throughout the brain suggesting differentiated physiological roles for each receptor subtype.[8] Selective expression of OX_2R in the histaminergic neurons in the tuberomammillary nucleus (TMN), which plays a critical role in promoting arousal, supports a primary role for OX_2R in the sleep-promoting effects of DORAs through the attenuation of histamine release.[9] Experiments in mice with targeted genetic ablation of both OXRs demonstrate that these dual-KO mice exhibit a narcoleptic phenotype similar to that of prepro-orexin KO animals lacking the ligand. Ablation of the single gene encoding OX_2R results in mice with a milder narcolepsy phenotype while OX_1R KO mice appear to have normal sleep/wake states without any obvious behavioral alterations.[10] Emerging literature suggests OX_1R antagonism has little influence on orexin-mediated arousal, but a more subtle role in vigilance state gating resulting in a lower threshold for sleep stage transitions, potentially influencing stage transitions and sleep onset.[11] Although antagonism of OX_1R has not been shown to result in overt sleep-promoting efficacy, many studies have implicated a role in the treatment of other conditions such as substance abuse, withdrawal, obesity and mood disorders.[8]

Clearly a need exists for the development of highly selective orexin receptor antagonists (SORAs) of OX_1R and OX_2R in order to better understand the underlying pharmacology of each receptor. Recent publications from our laboratories have disclosed the sleep-promoting effects of a novel triaryl 2-SORA structural class[12a] and a new DORA series derived from subtle changes to filorexant.[12b] Herein, we disclose a hybrid approach in which changes to the ether linkage and pendant heterocycle of filorexant impart significant selectivity for OX_2R, providing a novel piperidine ether 2-SORA series for evaluation of sleep-promoting effects.

Results and Discussion

Filorexant (Figure 2) is a potent antagonist of both human OX_1R and OX_2R as measured by a radioligand-displacement binding affinity assay (expressed as K_i values) and a fluorometric imaging plate reader (FLIPR) assay (expressed as IC_{50} values). The FLIPR assay provides a functional readout of orexin receptor antagonism in CHO cells engineered to overexpress the human receptors.[13] Filorexant has a low selectivity index (SI) of 9.[14] Importantly, it has demonstrated robust sleep efficacy in preclinical rat, dog,

and monkey models (decreased active wake, increased delta and REM sleep), and has recently achieved clinical proof of concept in human subjects.[15]

PLACE FIGURE 2 HERE.

Figure 2. Profile of filorexant.

Beginning with filorexant, we initially sought to alter the DORA structural framework to identify novel chemical space (Figure 3). Early SAR led us to return to the 2-triazolo moiety found in suvorexant. Additionally, to simplify our early synthetic efforts, we deleted the stereogenic methyl group on the piperidine core, with the assumption that any potency losses could be addressed by reinstallation of this group. Modification of the southeastern aromatic ring identified representative racemic compound **PE-1** bearing comparable selectivity and potency relative to filorexant. Truncation of the ether linkage by deletion of a single methylene group provided **PE-2**. While this compound lost absolute binding affinity, it led to an important structural modification that opened up new chemical space for the program. Replacement of the southeastern aromatic ring with a naphthyl group (**PE-3**) provided a significant improvement in binding affinity relative to **PE-2**, suggesting that biaryl substitutents would be favored in this series. Reinstallation of the stereogenic methyl group resulted in trans **±PE-4** that not only exhibited excellent OX_2R binding affinity, but also displayed a trend toward OX_2R selectivity (SI= 13). This result prompted us to continue optimization efforts within this structural class. Further structural modifications, including introduction of a nitrogen in the southeastern aromatic ring and deletion of the aromatic methyl group in the northwestern benzene ring, provided trans **±PE-5** with OX_2R selectivity further improved to SI= 35.

PLACE FIGURE 3 HERE.

Figure 3. Systematic progression of filorexant toward improved OX_2R selectivity.

With a promising core identified in **PE-5**, we initiated systematic optimization of the R1 and R2 positions with the goal of further improving OX_2R selectivity (Table 1). We learned quickly that the position of the southeastern arene nitrogen was crucial to compound selectivity. Walking the nitrogen around the bicyclic framework led to a steady improvement in OX_2R selectivity to SI= 397, imparted by a 4-quinoline moiety (Table 1, entries 1–6). For most of these compounds, however, this improved selectivity came at the expense of intrinsic OX_2R binding affinity. We next examined substitution about the 4-quinoline group (Table 1, entries 7–14) and discovered a significant steric and electronic impact of quinoline functionalization. A-ring substitution led universally to compromised binding affinity and selectivity, while improvements were realized upon substitution of the B-ring. Notably, halogen substituents at the 8-position provided additional improvements in both intrinsic OX_2R binding affinity and OX_2R selectivity, with a fluorine substituent being optimal. Resolution of the racemic 8-fluoro-4-quinoline analog identified (*R*,*R*) isomer **PE-6**, the most selective piperidine ether compound identified to date.

Table 1. Optimization and SAR of the piperidine ether framework.

PLACE TABLE 1 GRAPHIC HERE

Entry	R1	R2	hOX_2R K_i (nM)[a]	hOX_1R K_i (nM)	SI[b]
1 (PE-5)	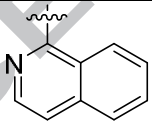 1-isoquinoline	2-(1,2,3-triazolo)	0.3	10.5	35
2	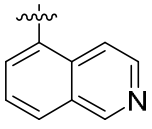 5-isoquinoline	2-(1,2,3-triazolo)	7.5	415	55
3	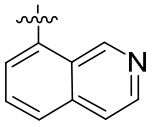 8-isoquinoline	2-(1,2,3-triazolo)	9.3	900	97

4	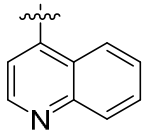 4-quinoline	2-(1,2,3-triazolo)	6.8	2700	397
5	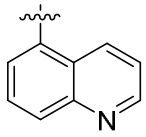 5-quinoline	2-(1,2,3-triazolo)	5.1	1030	202
6	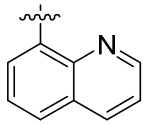 8-quinoline	2-(1,2,3-triazolo)	9.8	760	78
7	2-CH_3-4-quinoline	2-(1,2,3-triazolo)	28.9	3600	125
8	2-CF_3-4-quinoline	2-(1,2,3-triazolo)	149	-	-
9	3-Br-4-quinoline	2-(1,2,3-triazolo)	180	-	-
10	6-Br-4-quinoline	2-(1,2,3-triazolo)	5.2	470	90
11	8-Br-4-quinoline	2-(1,2,3-triazolo)	2.6	1100	423
12	8-Cl-4-quinoline	2-(1,2,3-triazolo)	0.9	510	567
13	8-F-4-quinoline	2-(1,2,3-triazolo)	1.3	910	700
14[c] **(PE-6)**	8-F-4-quinoline	2-(1,2,3-triazolo)	0.6	965	1608
15[c]	8-F-4-quinoline	3-pyridyl	63	19000	302
16[c]	8-F-4-quinoline	5-(1,2,4-triazolo)	1.1	1360	1236
17[c]	8-F-4-quinoline	2-pyrimidyl	0.8	1200	1500
18[c]	8-F-4-quinoline	$N(CH_3)_2$	370	-	-

[a] Binding K_i values were determined using a radioligand-displacement binding assay. Data presented are for racemates unless otherwise noted. [b]Selectivity index (SI) for OX_2R over OX_1R as calculated from the K_i. [c] Data presented for the more potent (*R*,*R*) enantiomer.

With an optimal eastern and central portion in place, we reinvestigated the southwestern R2 position (Table 1, Entries 14–18). While replacement of the 1,2,3-triazolo moiety with other arenes bearing multiple nitrogens (i.e. pyrimidine or 1,2,4-triazolo) was tolerated and maintained similar binding affinity and OX_2R selectivity to **PE-6**, more dramatic functional alterations resulted in decreased OX_2R selectivity through significant loss in OX_2R binding affinity. We ultimately selected **PE-6** for further characterization as the lead compound from this novel structural class.

The 1st generation racemic synthesis of **PE-6** is highlighted in Scheme 1. RuO_2-catalyzed homogenous hydrogenation of 2-methyl-5-hydroxypyridine under highly forcing conditions provides a mixture of the racemic cis and trans diastereomers of key piperidine building block **1**. Unfortunately, under these conditions, the desired cis diastereomer is formed as the *minor* component, in a >4:1 diasteromeric ratio. Standard amide coupling provides **3**, which then undergoes a Mitosunobu reaction with 8-fluoro-4-hydroxyquinoine and a subsequent separation on chiral stationary phase to provide **PE-6** in <2% overall yield from mixture **1.**

PLACE SCHEME 1 HERE.

Scheme 1. 1st generation synthesis of **PE-6**.

Given the very low yields and racemic nature of the above route, we sought to develop an enantioselective synthesis of **PE-6** while improving the efficiency of overall synthetic sequence. Scheme 2 highlights our 2nd generation route. The sequence begins with CoSalen-catalyzed hydrolytic kinetic resolution (HKR) of hexene-1-oxide to provide **4**.[16] Employing a unique substrate-controlled reverse-Cope cyclization,[17] reasonable yields of cis benzyl-piperidine-*N*-oxide **5** were obtained in high ee following slight modification of the published procedure. Silylation to **6** followed by hydrogenolysis to **7** furnished a protected form of our key chiral piperidine building block. We discovered that incorporation of the silyl group facilitated a higher yielding amide coupling. To this end, coupling of **7** and **2**, followed by removal of the protecting group, and finally a Mitsunobu reaction with 8-fluoro-4-hydroxyquinoline furnished the desired cis enantiomer of **PE-6** in 60% overall yield from single enantiomer **7**, a significant improvement over our original route.

PLACE SCHEME 2 HERE.

Scheme 2. Enantioselective synthesis of key chiral building block **7** and elaboration to **PE-6**.

While numerous functionalized 4-hydroxyquinolines are commercially-available, our lead optimization efforts required access to variants of this aromatic core. In order to

gain efficient access to novel building blocks, we optimized a known protocol to facilitate a 1-pot synthesis.[18] In this sequence, Meldrum's acid was initially treated with triethylorthoformate under forcing conditions to form intermediate **int-8**, which was treated *in situ* with functionalized aniline of choice to provide carboxy-quinolone **8**. The reaction mixture was subsequently diluted with diphenylether in an open vessel and heated to 270 ℃ to effect the desired decarboxylation to **9**. Upon cooling and trituration with diethyl ether, **9** could be isolated by a simple filtration.

PLACE SCHEME 3 HERE.

Scheme 3. 1-pot synthesis of non-commercial 4-hydroxyquinolines.

PE-6 is a highly selective 2-SORA displaying in vitro OX_2R potency comparable to filorexant, with 1608-fold and 217-fold selectivities in binding affinity and FLIPR potency, respectively (Figure 4). It has favorable physicochemical properties with an HPLC LogD of 2.35, 3–4% free fraction in human and rat plasma, and an aqueous solubility of 161 μM at neutral pH. **PE-6** was not a potent reversible inhibitor of CYP3A4, 2D6 or 2C9, (IC_{50}= 25.4 μM, >50 μM and 21.4 μM, respectively) and was also not a time-dependent inhibitor of CYP3A4. **PE-6** is highly selective only for OX_2R, showing no significant off-target activities when screened against a Panlabs panel (165 assays) of receptor and enzyme targets with melatonin identified as the only activity of note (K_i >5 μM) representing a greater than 5000-fold margin over OX_2R binding affinity.

PLACE FIGURE 4 HERE.

Figure 4. Profile of **PE-6**.

The pharmacokinetics of **PE-6** in Sprague–Dawley rats and beagle dogs are reported in Table 2. After intravenous administration, **PE-6** exhibited low-to-moderate clearance and a short terminal half-life in both species. The oral bioavailability was 60% in dogs and 19–50% in rats, with peak plasma concentrations achieved rapidly in both species

Table 2. Pharmacokinetics of compound **PE-6** in rat and dog.

Species	Intravenous (IV) administration			Oral (PO) administration				
	Dose [mg/kg]	Cl [mL/min/kg]	$t_{1/2}$ [h]	Dose [mg/kg]	AUC [μM•h]	C_{max} [μM]	T_{max} [h]	F [%]
Rat	2	22.5	0.4	10	3.9			19
Rat				30	30.1	15.7	0.5	50
Dog	0.125	6.2	0.7	3	16	5.65	0.38	60

PE-6 achieved 72% receptor occupancy at a plasma level of 9.5 μM after a 30 mg/kg oral dose (t= 30 min) to rats.[19] At this dose, levels in the CSF were low at 339 nM, which is consistent with the fact that **PE-6** is a substrate for rat P-glycoprotein (Pgp), with a basaolateral-apical to apical-basolateral (B-A/A-B) ratio of 5.8. Given its high passive permeability (P_{app}= 34 x 10^{-6} cm/s) and a lower B-A/A-B ratio (2.5) in the human Pgp transporter assay, we chose to advance **PE-6** into EEG-telemetry studies to evaluate sleep efficacy.

PE-6 administered orally to rats at 30 mg/kg significantly attenuated active wake relative to vehicle (20% vitamin E TPGS) for 30 minutes following treatment (Figure 5). These changes were accompanied by sleep promotion characterized by increases in both delta and REM sleep, although the effect on the latter was modest. Qualitatively, these changes in sleep architecture are similar not only to filorexant and other DORAs, but also to MK-1064, a 2-SORA evaluated in our laboratory, where increases in both delta and REM sleep have been observed.[12a] From an efficacy standpoint, the responses to 30 mg/kg **PE-6** are shorter-lived and diminished in magnitude relative to those observed for filorexant, which exhibits similar *in vitro* potency toward OX_2R,[13a,20] the receptor primarily responsible for the sleep promoting effects of orexin receptor antagonists.[9] While differences in OX_1R selectivity between **PE-6** and filorexant are potentially involved, direct efficacy comparisons with filorexant are not appropriate given the shorter half-life of **PE-6** and the increased Pgp efflux of this compound. Future studies describing the differential effects of OX_1R and OX_2R antagonism on sleep efficacy will need to evaluate multiple DORAs and SORAs with sleep-promoting effects that have been normalized for target engagement to account for compound-specific differences in pharmacokinetics and brain exposure.

PLACE FIGURE 5 HERE.

Figure 5. Proportional sleep induced by **PE-6**. Mean time in active wake, light sleep, delta sleep and REM sleep in rats during oral administration of 30 mg/kg of **PE-6** (open symbols) or vehicle (20% vitamin E TPGS, closed circles) monitored for 30 min prior and 2 h post-dose. Treatment occurred during the active phase at 09:00 (ZT [Zeitgeber Time] 17:00; 7 h prior to lights on) indicated by the gray vertical bar. Data shown are mean values in 10 minute intervals (-SEM) from 3 consecutive days of treatment administered in a balanced cross-over design such that each subject received drug and vehicle (N=6). Compound condition was compared to vehicle using a mixed-model ANOVA applied within subjects at each time point in the R statistical computing environment (version 3.0.1, cran.us.r-project.org; the R Foundation for Statistical Computing, Vienna, Austria) and significance determined using a linear mixed effects model. Significant differences between mean conditions at each time point are indicated by grey vertical lines and significance level by tick marks at the top of each graph (short, medium, long; $p < 0.05$, 0.01, 0.001).

Through the course of the lead optimization efforts in the piperidine ether series described above, we identified compounds that span the orexin selectivity spectrum from DORA to 2-SORA. Additional efforts from our laboratories have subsequently identified structurally related piperidine ether 1-SORAs, which will be the subject of a forthcoming manuscript. Three representative molecules are highlighted in Figure 6. By replacing the fluoroquinoline of 2-SORA **PE-6** with a 4-methoxyisoquinoline, OX_1R potency is restored providing **PE-7**, an extremely potent DORA with SI <2. Conversely, replacement of the 2-methylpiperidine with a 4,4-difluroropiperidine and alteration of the arene connectivity completely reverses orexin receptor selectivity, and provides **PE-8**, a potent 1-SORA with an OX_1R SI= 434.[21] This degree of "tunable" diversity in orexin receptor selectivity from a single structural class highlights a unique opportunity to employ piperidine ether orexin receptor antagonists as tools to further interrogate the biology and pharmacology of the orexin signaling pathway. These studies are on-going,

and will be reported in due course. Importantly, the significant changes in receptor selectivity imparted by subtle alterations in compound structure in the piperidine ether series underscore the challenges associated with the rational design of SORAs resulting from a lack of understanding of the origin of their selectivity.[22]

PLACE FIGURE 6 HERE.

Figure 6. Representative 2-SORA, DORA, and 1-SORA piperdine ethers highlighting the wide selectivity range attainable by this compound class.

In summary, we have described the discovery of a novel class of piperidine ether 2-SORAs obtained by systematic modification of the clinically validated filorexant series. These modifications include truncation of the ether linkage and incorporation of bicyclic heterocycles that impart selectivity for the orexin 2 receptor. Additional changes to the western amide resulted in the identification of **PE-6**, displaying sub-nanomolar binding affinity for OX_2R with >1600-fold binding selectivity over OX_1R. **PE-6** significantly attenuated active wake and promoted sleep in rats after oral dosing in a manner qualitatively similar to filorexant. Subtle alterations to the bicyclic heterocycle and/or the piperidine core have resulted in the identification of very potent DORA and 1-SORA molecules from the same piperidine ether series. Access to a range of orexin selectivities from a single structural class provides a unique set of tool molecules to help further interrogate the underlying pharmacology of the orexin signaling pathway.

Acknowledgements

The authors thank the Merck West Point NMR and Mass Spectrometry facilities for assistance in characterizing the compounds presented in this manuscript.

References

1. de Lecea, L.; Kilduff, T. S.; Peyron, C.; Gao, X. B.; Foye, P. E.; Danielson, P. E.; Fukuhara, C.; Battenberg, E. L. F.; Gautvik, V. T.; Bartlett, F. S.; Frankel, W. N.;

van den Pol, A. N.; Bloom, F. E.; Gautvik, K. M.; Sutcliffe, J. G. *PNAS* **1998**, *95*, 322.

2. Sakurai, T.; Amemiya, A.; Ishii, M.; Matsuzaki, I.; Chemelli, R. M.; Tanaka, H.; Williams, S. C.; Richardson, J. A.; Kozlowski, G. P.; Wilson, S.; Arch, J. R. S.; Buckingham, R. E.; Haynes, A. C.; Carr, S. A.; Annan, R. S.; McNulty, D. E.; Liu, W. S.; Terrett, J. A.; Elshourbagy, N. A.; Bergsma, D. J.; Yanagisawa, M. *Cell* **1998**, *92*, 573.
3. Lin, L.; Faraco, J.; Li, R.; Kadotani, H.; Rogers, W.; Lin, X.; Qiu, X.; de Jong, P. J.; Nishino, S.; Mignot, E. *Cell*, **1999**, *98*, 365.
4. Chemelli, R. M.; Willie, J. T.; Sinton, C. M.; Elmquist, J. K.; Scammell, T.; Lee, C.; Richardson, J. A.; Williams, S. C.; Xiong, Y. Kisanuki, Y.; Fitch, T. E.; Nakazato, M,; Hammer, R. E.; Saper, C. B.; Yanagisawa, M. *Cell*, **1999**, *98*, 437.
5. Thannickal, T. C.; Moore, R. Y.; Nienhuis, R.; Ramanathan, S.; Gulyani, S.; Aldrich, M.; Cornford, M.; Siegel, J. M. *Neuron*, **2000**, *27*, 469.
6. Coleman, P. J.; Schreier, J. D.; Cox, C. D.; Breslin, M. J.; Whitman, D. B.; Bogusky, M. J.; McGaughey, G. B.; Bednar, R. A.; Lemaire, W.; Doran, S. M.; Fox, S. V.; Garson, S. L.; Gotter, A. L.; Harrell, C. M.; reiss, D. R.; Cabalu, T. D.; Cui, D.; Prueksaritanont, T.; Stevens, J.; Tannenbaum, P. L.; Ball, R. G.; Stellabott, J.; Young, S. D.; Hartmann, G. D.; Winrow, C. J.; Renger, J.J. *ChemMedChem*, **2012**, *7*, 415.
7. (a) Brisbare-Roch, C.; Dingemanse, J.; Koberstein, R.; Hoever, P.; Aissaoui, H.; Flores, S.; Mueller, C.; Nayler, O.; van Gerven, J.; de Haas, S. L.; Hess, P.; Qiu, C.; Buchmann, S.; Scherz, M.; Weller, T.; Fischli, W.; Clozel, M.; Jenck, F. *Nature Medicine*. **2007**, *13*, 150. (b) Gatfield, J.; Brisbare-Roch, C.; Jenck, F.; Boss, C. *ChemMedChem*. **2010**, *5*, 1197. (c) Lebold, T. P.; Bonaventure, P.; Shireman, B. T. *Bioorg. Med. Chem. Lett.* **2013**, *23*, 4761.
8. Tsujino, N.; Sakurai, T. *Pharmacol Rev*, **2009**, *61*, 162.
9. Gotter, A. L., Webber, A. L., Coleman, P. J., Renger, J. J., Winrow, C. J. *Pharmacol. Rev.*, **2012**, 64, 389.

10. Kohlmeier, K. A.; Tyler, C. J.; Kalogiannis, M.; Ishibashi, M.; Kristensen, M. P.; Gumenchuk, I.; Chemelli, R. M.; Kisanuki, Y. Y.; Yanagisawa, M.; Leonard, C. S. *Front. Neurosci*., **2013**, *7*, 246.
11. Mieda, M., Hasegawa, E., Kisanuki, Y. Y., Sinton, C. M., Yanagisawa, M., Sakurai, T. *J. Neurosci*., **2011**, *31*, 6518.
12. (a) Roecker, A. J.; Mercer, S. P.; Schreier, J. D.; Cox, C. D.; Fraley, M. E.; Steen, J. T.; Lemaire, W.; Bruno, J. G.; Harrell, C. M.; Garson, S. L.; Gotter, A. L.; Fox, S. V.; Stevens, J.; Tannenbaum, P. L.; Prueksaritanont, T.; Cabalu, T. D.; Cui, D.; Stellabott, J.; Hartman, G. D.; Young, S. D.; Winrow, C. J.; Renger, J. J.; Coleman, P. J. *ChemMedChem*, **2014**, *9*, 311. (b) Kuduk, S. D.; Skudlarek, J. W.; DiMarco, C. N.; Bruno, J. G.; Pausch, M. A.; O'Brien, J. A.; Cabalu, T. D.; Stevens, J.; Brunner, J.; Tannenbaum, P. L.; Gotter, A. L.; Winrow, C. J.; Renger, J. J.; Coleman, P. J. *Bioorg. Med. Chem. Lett.* **2014**, 24, 1784.
13. (a) Winrow, C. J.; Gotter, A. L.; Cox, C. D.; Doran, S. M.; Tannenbaum, P. L.; Breslin, M. J.; Garson, S. L.; Fox, S. V.; Harrell, C. M.; Stevens, J.; Reiss, D. R.; Cui, D.; Coleman, P. J.; Renger, J. J. *J Neurogenet.* **2011**, *25*, 52. (b) Cox, C. D.; Breslin, M. J.; McGaughey, G. B.; Whitman, D. B.; Schreier, J. D.; Bogusky, M. J.; Roecker, A. J.; Mercer, S. P.; Bednar, R. A.; Lemaire, W.; Bruno, J. G.; Reiss, D. R.; Harrell, C. M.; Murphy, K. L.; Garson, S. L.; Doran, S. M.; Koblan, K. S.; Prueksaritanont, T.; Anderson, W. B.; Tang, C.; Roller, S.; Cabalu, T. D.; Cui, D.; Ball, R. G.; Hartman, G. D.; Winrow, C. J.; Renger, J. J.; Coleman, P. J. *J. Med. Chem.* **2010**, *53*, 5320.
14. SI= hOX_1R K_i / hOX_2R K_i
15. Connor, K.M. "A Dual Orexin Receptor Antagonist, MK-6096, in Patients with Primary Insomnia: Randomized, Controlled, Crossover Polysomnography Study." Presented at the World Sleep Congress, Kyoto, Japan, **2011**. Talk# PO-1-236.
16. Nielsen, L. P. C.; Stevenson, C. P.; Blackmond, D. G.; Jacobsen, E. N. *J. Am. Chem. Soc.* **2004***, 126,* 1360.
17. O'Neil, I. A., Cleator, E., Southern, J. M., Hone, N., Topolczay, D.J. *Synlett*., **2000**, *5*, 695

18. Margolis, B. J.; Long, K. A.; Laird D. L. T.; Ruble, J. C.; Pulley, S. R. *J. Org. Chem.* **2007***, 72,* 2232.
19. Gotter, A. L.; Winrow, C. J.; Brunner, J.; Garson, S. L.; Fox, S. V.; Binns, J.; Harrell, C. M.; Cui, D.; Yee, K. L.; Stiteler, M.; Stevens, J.; Savitz, A.; Tannenbaum, P. L.; Tye, S. J.; McDonald, T.; Yao, L.; Kuduk, S. D.; Uslaner, J.; Coleman, P. J.; Renger, J. J. *BMC Neuroscience.* **2013,** *14*, 1.
20. Winrow, C. J.; Gotter, A. L.; Cox, C. D.; Tannenbaum, P. L.; Garson, S. L.; Doran, S. M.; Breslin, M. J.; Schreier, J. D.; Fox, S. V.; Harrell, C. M.; Stevens, J.; Reiss, D. R.; Cui, D.; Coleman, P. J.; Renger, J. J. *Neuropharmacology*. **2012**, *62*, 978.
21. Patent Application **WO 2014/113303 A1**; published July 24, 2014.
22. McGaughey, G.; Bayly, C. I.; Cox, C. D.; Schreier, J. D.; Breslin, M. J.; Bogusky, M. J.; Pitzenberger, S.; Ball, R.; Coleman, P. J. *J. Comput. Aided Mol. Des.* **2014**, *28*, 5.

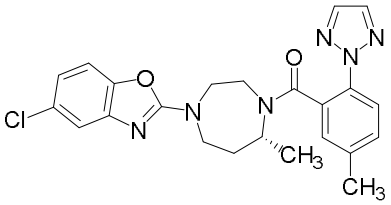

Suvorexant

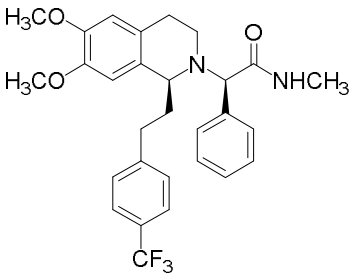

Almorexant

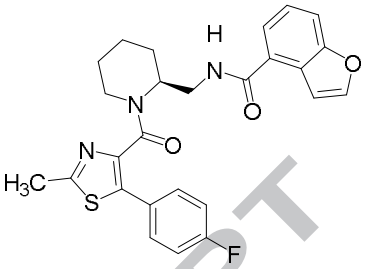

SB-649868

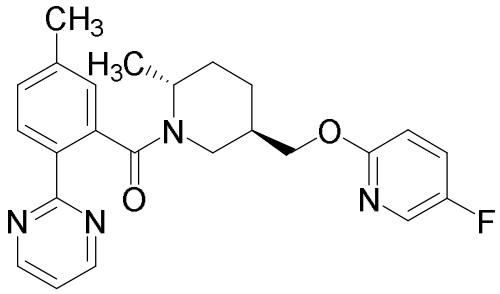

Filorexant

hOX_2R Ki= 0.3 nM

hOX_1R Ki= 2.9 nM

hOX_2R FLIPR IC_{50}= 17 nM

hOX_1R FLIPR IC_{50}= 16 nM

SI: 9

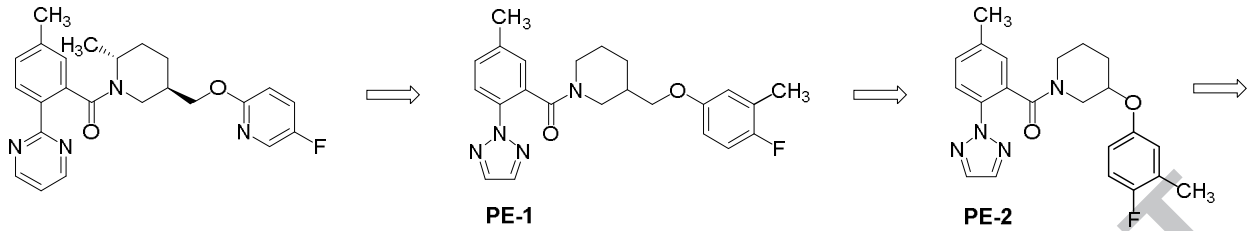

PE-1
hOX_2R Ki= 8.9 nM
hOX_1R Ki= 5.5 nM
SI= 0.6

PE-2
hOX_2R Ki= 55 nM
hOX_1R Ki= 106 nM
SI= 2

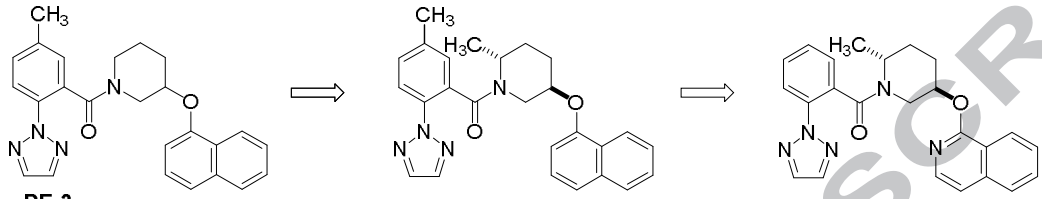

PE-3
hOX_2R Ki= 18 nM
hOX_1R Ki= 9 nM
SI= 0.5

PE-4
hOX_2R Ki= 1.0 nM
hOX_1R Ki= 13 nM
SI= 13

PE-5
hOX_2R Ki= 0.3 nM
hOX_1R Ki= 10.5 nM
SI= 35

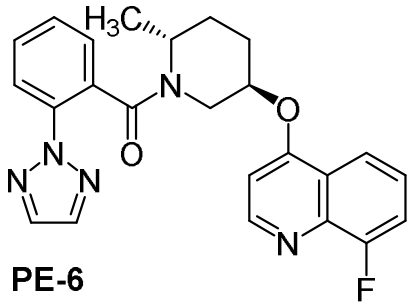

PE-6

hOX_2R Ki= 0.6 nM

hOX_1R Ki= 965 nM

hOX_2R FLIPR IC_{50}= 18 nM

hOX_1R FLIPR IC_{50}= 3908 nM

SI: 1608

PPB (h, r)= 97.1, 96%

Solubility (pH 2, 7)= 182, 161 μM

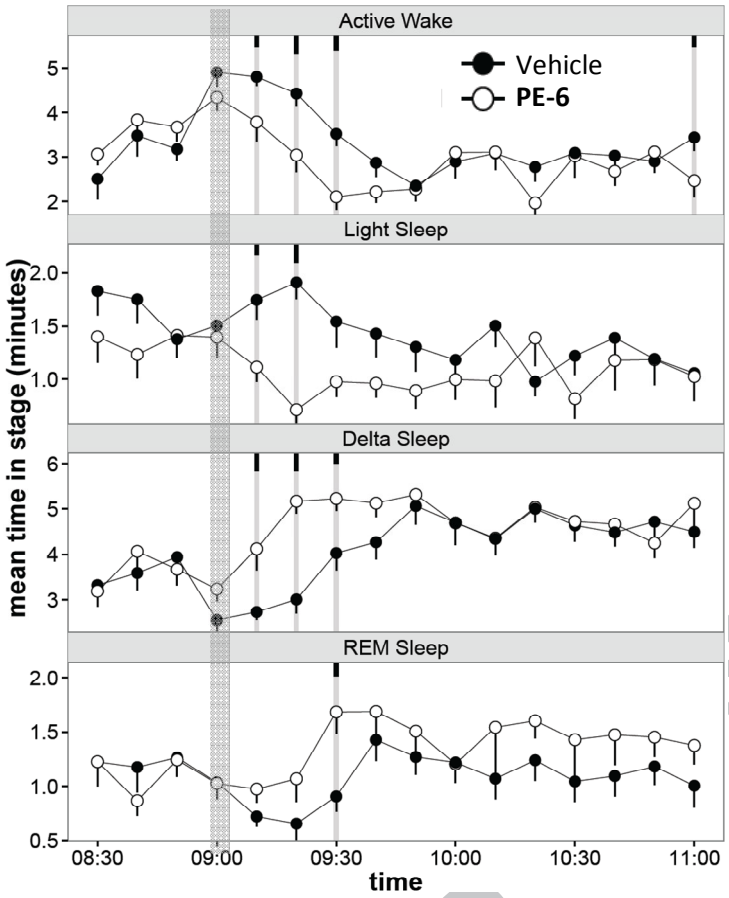

2-SORA

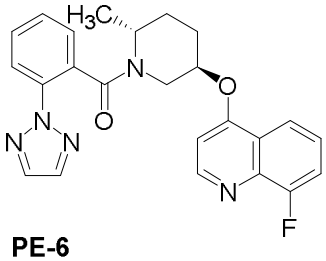

PE-6
hOX_2R Ki= 0.6 nM
hOX_1R Ki= 965 nM

OX_2R selectivity ⟷

DORA

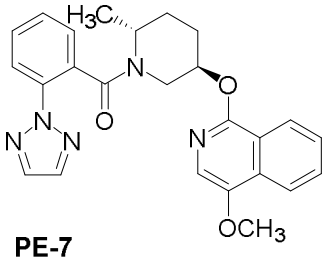

PE-7
hOX_2R Ki= 0.24 nM
hOX_1R Ki= 0.41 nM

OX_1R selectivity ⟷

1-SORA

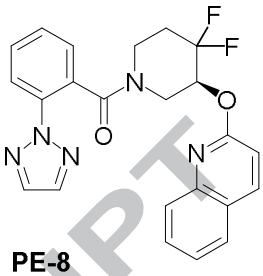

PE-8
hOX_2R Ki= 521 nM
hOX_1R Ki= 1.3 nM

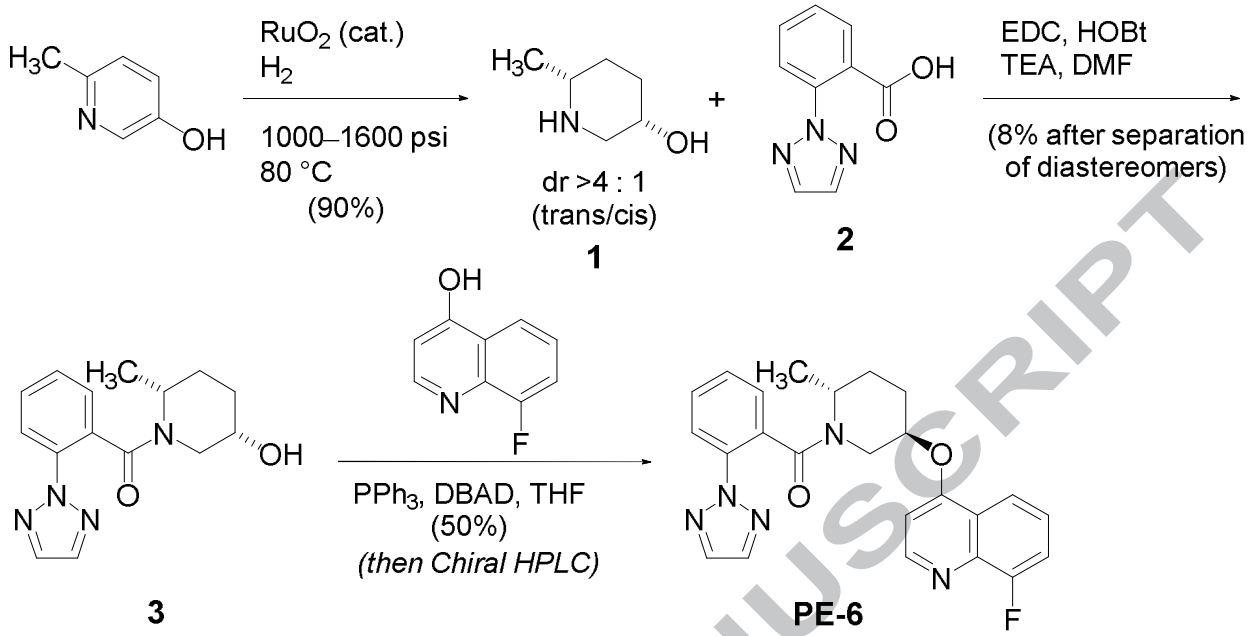

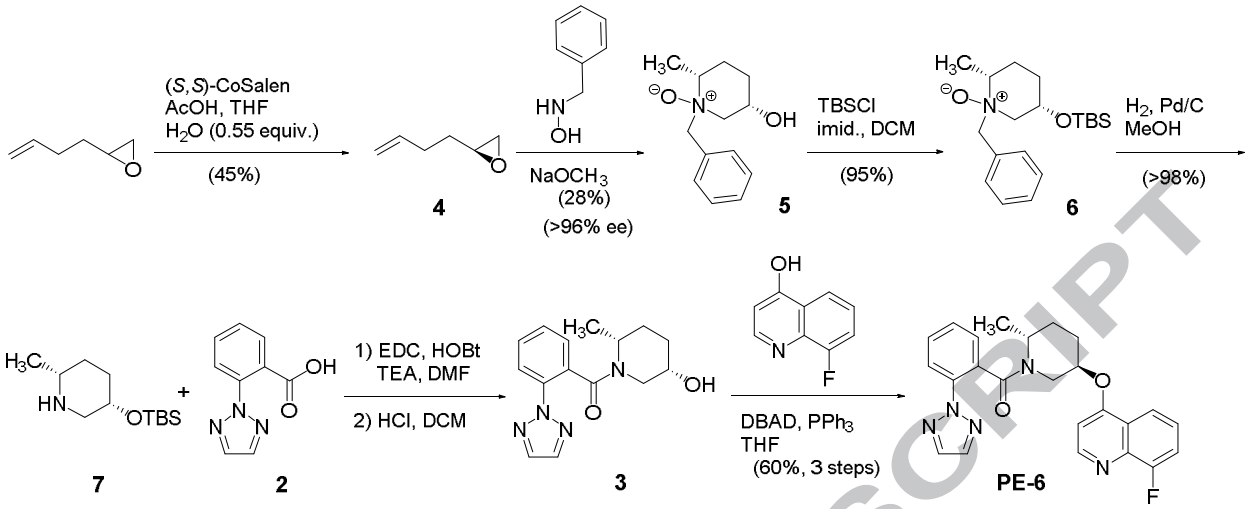

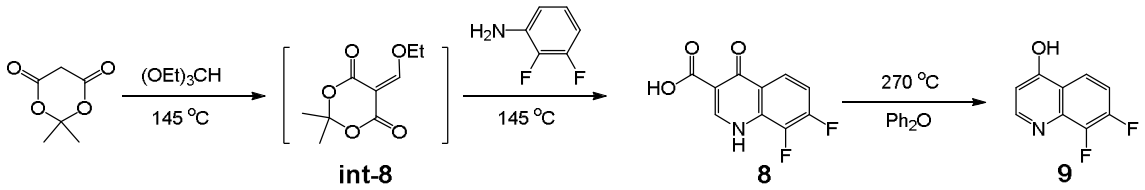

Discovery of Piperidine Ethers as Selective Orexin Receptor Antagonists (SORAs) Inspired by Filorexant

Izzat T. Raheem,[a] Michael J. Breslin,[a] Joseph Bruno,[e] Tamara D. Cabalu,[c] Andrew Cooke,[a] Christopher D. Cox,[a] Donghui Cui,[c] Susan Garson,[b] Anthony L. Gotter,[b] Steven V. Fox,[d] C. Meacham Harrell,[b] Scott D. Kuduk,[a] Wei Lemaire,[e] Thomayant Prueksaritanont,[c] John J. Renger,[b] Craig Stump,[a] Pamela L. Tannenbaum,[d] Peter D. Williams,[a] Christopher J. Winrow,[b] and Paul J. Coleman.[a]

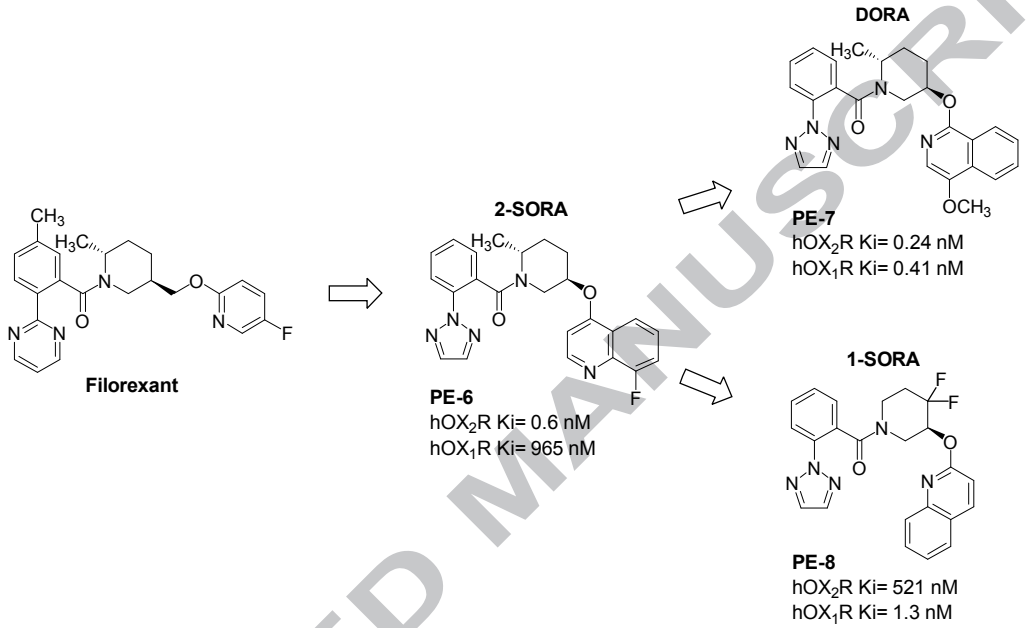

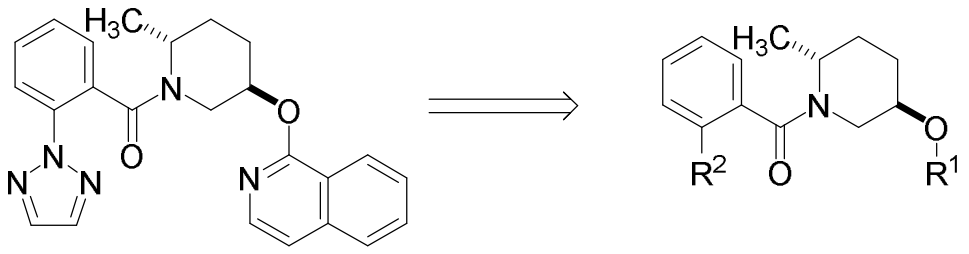

PE-5